



Provided by the author(s) and NUI Galway in accordance with publisher policies. Please cite the published version when available.

Title	Monitoring cell culture media degradation using surface enhanced Raman scattering (SERS) spectroscopy
Author(s)	Calvet, Amandine; Ryder, Alan G.
Publication Date	2014-06-13
Publication Information	Calvet, A,Ryder, AG (2014) 'Monitoring cell culture media degradation using surface enhanced Raman scattering (SERS) spectroscopy'. <i>Analytica chimica acta</i> , 840 :58-67.
Publisher	Elsevier (Science Direct)
Link to publisher's version	<a href="http://dx.doi.org/10.1016/j.aca.2014.06.021">http://dx.doi.org/10.1016/j.aca.2014.06.021</a>
Item record	<a href="http://hdl.handle.net/10379/4824">http://hdl.handle.net/10379/4824</a>
DOI	<a href="http://dx.doi.org/10.1016/j.aca.2014.06.021">http://dx.doi.org/10.1016/j.aca.2014.06.021</a>

Downloaded 2019-01-19T15:23:43Z

Some rights reserved. For more information, please see the item record link above.



# 1 **Monitoring Cell Culture Media Degradation using Surface** 2 **Enhanced Raman Scattering (SERS) Spectroscopy.**

3  
4 Amandine Calvet and Alan G. Ryder. \*

5 Nanoscale Biophotonics Laboratory, School of Chemistry, National University of Ireland,  
6 Galway, Galway, Ireland

7 \* Corresponding author: **Email:** alan.ryder@nuigalway.ie **Phone:** +353-91-492943.

8 **Postal address:** Nanoscale Biophotonics Laboratory, School of Chemistry, National  
9 University of Ireland, Galway, University Road, Galway, Ireland.

10  
11 **Note:** This is the author version of the paper, the final published version DOI is:  
12 [10.1016/j.aca.2014.06.021](https://doi.org/10.1016/j.aca.2014.06.021)

## 13 14 15 **Abstract:**

16 The quality of the cell culture media used in biopharmaceutical manufacturing is a crucial  
17 factor affecting bioprocess performance and the quality of the final product. Due to their  
18 complex composition these media are inherently unstable, and significant compositional  
19 variations can occur particularly when in the prepared liquid state. For example photo-  
20 degradation of cell culture media can have adverse effects on cell viability and thus process  
21 performance. There is thus, from quality control, quality assurance and process management  
22 view points, an urgent demand for the development of rapid and inexpensive tools for the  
23 stability monitoring of these complex mixtures. Spectroscopic methods, based on  
24 fluorescence or Raman measurements, have now become viable alternatives to more time-  
25 consuming and expensive (on a unit analysis cost) chromatographic and/or mass  
26 spectrometry based methods for routine analysis of media. Here we demonstrate the  
27 application of Surface Enhanced Raman Scattering (SERS) spectroscopy for the simple, fast,  
28 analysis of cell culture media degradation. Once stringent reproducibility controls are  
29 implemented, chemometric data analysis methods can then be used to rapidly monitor the  
30 compositional changes in chemically defined media. SERS shows clearly that even when  
31 media are stored at low temperature (2-8 °C) and in the dark, significant chemical changes  
32 occur, particularly with regard to cysteine/cystine concentration.

33  
34 **Keywords:** Raman spectroscopy, Surface Enhanced Raman Scattering (SERS),  
35 Biotechnology, cell culture media, photo-degradation, chemometrics.

## 36 37 38 **1. Introduction**

39 Cell culture media are an essential part of industrial mammalian cell culture,  
40 sustaining optimal cell growth and ensuring correct product formation. In many cases  
41 chemically defined (CD) media are now being used to avoid inconsistency issues associated  
42 with complex hydrolysates and other biologically derived media. CD media are usually  
43 complex aqueous chemical mixtures containing a range of amino acids, carbohydrates,  
Page 1 of 19

44 vitamins, inorganic salts and other supplements. One such example is eRDF, an enriched  
45 basal RDF medium containing higher amino acids and glucose concentrations which has ~60  
46 components [1]. Media quality is absolutely critical to process performance, reliability, and  
47 reproducibility. However, it is known that media are not chemically stable [2] and undergo  
48 some slow rate chemical reactions when stored in the dark between 2-8 °C, the industry norm  
49 for storing liquid cell culture media. It is also well known that chemical changes induced by  
50 light exposure can adversely affect process performances and cell viability [2-8]. In addition,  
51 some unstable components like cysteine are of particular interest since it and its oxidation  
52 product, cystine, can have significant effects on protein aggregation [9]. Therefore it is  
53 critical importance to assess and monitor media stability particularly during process  
54 development where unknown/uncontrolled media variability can have very adverse  
55 consequences. Multi-dimensional fluorescence in combination with chemometric data  
56 analysis has been used to easily monitor light induced changes in media like eRDF [10, 11].  
57 This was possible due to the fact that riboflavin and some of the significant photoactive  
58 compounds (Tryptophan / Tyrosine) in the media are fluorescent. Furthermore, several  
59 photoproducts were also fluorescent and so by use of chemometric tools like PARAFAC [12]  
60 and MCR [13] it was possible to track composition changes. However this technique was not  
61 able to detect changes affecting non-fluorescent original components or degradation products.

62 The use of Raman spectroscopy for media analysis can lead to a more comprehensive  
63 analysis of the media composition because nearly all molecular constituents of media have  
64 distinct Raman spectra and can easily be distinguished [14, 15]. Unfortunately, conventional  
65 Raman spectroscopy is not good for analytes present in low concentration (<~0.5% w/w)  
66 which is the case in most components in liquid cell culture media. One way in which  
67 sensitivity can be enhanced is to use Surface Enhanced Raman Scattering (SERS) [16-18].  
68 SERS is the enhancement effect on Raman scattering observed when molecules are adsorbed  
69 onto nanosized noble metal structures, typically fabricated from gold or silver. SERS is  
70 potentially a very sensitive analytical method (down to single molecule) for complex  
71 biogenic materials analysis [16, 19, 20]. SERS measurements could provide valuable  
72 information about variances in media in terms of the non-fluorescing components which  
73 would then complement existing fluorescence EEM based measurements [2, 11, 19, 21, 22].

74 Here we show how SERS in combination with chemometric methods can be used to  
75 rapidly identify and monitor chemical changes in cell culture media under different storage  
76 conditions. However SERS is fundamentally difficult to implement reproducibly and thus  
77 careful experimental design and a high degree of care was required during the experimental  
78 work to ensure that the SERS data was both correct and reproducible. It was for this reason  
79 that a silver colloid SERS substrate was used, and additionally because it avoided  
80 carbonization problems that can be an issue with solid substrates. This method provided a  
81 rapid, simple, and inexpensive approach for media monitoring over extended timeframes,  
82 which should be of benefit for industrial biotechnology.

83

## 84 **2. Materials and methods**

85

86 2.1 *Materials:* eRDF was obtained from Kyokuto Pharmaceuticals Industrial (Japan).  
87 Sodium bicarbonate (>99.7 %), silver nitrate (99.999 % metal basis), sodium citrate (>99.0  
88 %) were obtained from Sigma-Aldrich and used without further purification. eRDF stock  
89 solution ( $17.7 \text{ g L}^{-1}$ ) was prepared by dissolving 4.4248 g of eRDF powder and 0.2832 g of  
90 sodium bicarbonate in  $250 \text{ cm}^3$  of sterilized high purity water. The solution was immediately  
91 sterilized by membrane ( $0.22 \mu\text{m}$ ) filtration and then dispensed (1.25 mL aliquots) into sterile  
92 2 mL translucent polypropylene eppendorf tubes before being placed in one of the four  
93 storage conditions: 1). RT-L: Room temperature ( $16.4 \pm 3.0 \text{ }^\circ\text{C}$ ) in the light; 2). RT-D:  
94 Room temperature in the dark; 3). C-L: Cold (Fridge,  $6.0 \pm 1.5 \text{ }^\circ\text{C}$ ) with light, and 4). C-D:  
95 Cold (Fridge) in the dark. All other details have been communicated previously [11]. SERS  
96 data were collected over 32 days (Day 0, 7, 11, 14, 18, 21, 25, 28, and 32). At every  
97 sampling point three samples were removed from each storage condition and immediately  
98 placed in the dark at  $4^\circ\text{C}$  to limit any further change in the samples during data acquisition.

99

100 2.2 *SERS, Raman Instrumentation, and data collection:* Silver colloid was carefully prepared  
101 using the Lee and Meisel method [10, 18]. Prior to preparation all glassware was thoroughly  
102 washed firstly with soap, rinsed with high purity water (HPW) from a Milli-Q® system, then  
103 isopropanol, HPW, and then soaked overnight in *aqua regia* before being rinsed again with  
104 HPW, until the pH of the rinsing water was neutral (pH paper). If multiple batches of colloid  
105 were being prepared over a week, the glassware was only rinsed with HPW between batches.  
106 Batches produced straight after cleaning of the glassware with *aqua regia* were  
107 systematically discarded as they had a wider particle size distribution and larger mean size.  
108 This effect was probably due to glass surface modification during cleaning, which changed  
109 the dynamics of nanoparticle formation. Subsequent batches made in the same glassware  
110 immediately afterwards, without cleaning, showed more consistent physical and SERS  
111 properties.

112 A silver nitrate solution was first prepared by dissolving 45 mg of  $\text{AgNO}_3$  in 250 mL of HPW  
113 and brought to the boil. When the temperature of the paraffin bath reached  $135 \text{ }^\circ\text{C}$ , 5mL of  
114 1% sodium citrate (57 mg in 5mL HPW) was slowly ( $\sim 1$  drop every 4s) introduced to the  
115 boiling solution using a pressure equalizing dropping funnel. The reflux was maintained for  
116 1 hour and the system was protected from the light at all times using aluminum foil. In  
117 practice, a color change, from clear and colorless to opaque olive/grey, rapidly after the start  
118 of the citrate addition indicates a successful preparation (absorbance maximum around 404  
119 nm and full width half maximum of the absorbance  $< 100 \text{ nm}$ , see below).

120 UV-vis spectroscopy was used as the primary quality assurance tool as both the maximum of  
121 the Plasmon resonance and the FWHM of the absorption band are symptomatic of both  
122 nanoparticle size and distribution [23, 24]. Ideally, these measurements should be validated  
123 using particle size measurements at the same time, but this was not available in this instance.  
124 There are several published studies correlating both size and size-distribution with the UV-vis  
125 spectroscopic studies, both experimentally and from a theoretical standpoint.

126 Using this approach, reasonably reproducible colloid quality was achieved with an average  
127 absorbance maximum ( $\lambda_{\text{max}}$ ) and full width half maximum (FWHM) of  $404 \pm 2.5 \text{ nm}$  and  
128  $86 \pm 15 \text{ nm}$  respectively (for the six batches used in this study). Batches 7 and 8 were

129 combined for this study, and this mixture was characterised by a FWHM = 86 nm and a  $\lambda_{\max}$   
130 (abs.) = 404 nm, which suggests an average particle size of ~20 nm [24-26]. While, the  
131 particle size is smaller than the 50 nm optimum for 785 nm excitation (in terms of SERS  
132 enhancement) as determined by Stampelcoskie *et al.* [26], it was appropriate for this  
133 application where signal reproducibility rather than enhancement factor was the critical issue.  
134 The only change observed between follow-on batches was a varying baseline in the Raman  
135 spectra of the pure colloid probably due to small changes in the particle size distribution (*see*  
136 *supplemental information, SI*). Finally, each colloid batch was contamination checked by  
137 Raman analysis immediately prior to use.

138 SERS spectra were collected with 785 nm excitation (1 sec. exposure, 8 cm<sup>-1</sup> resolution)  
139 using a RamanStation spectrometer (AVALON Instruments Ltd., Belfast) on 100 $\mu$ L sample  
140 volumes in a stainless steel wellplate [14]. The effect of sample to colloid ratio (SC ratio)  
141 and incubation time on the quality of the SERS spectra were investigated (*data not shown*,  
142 [10]). Ultimately, a 1:19 SC ratio was selected (*vide infra*) and every test sample consisted of  
143 5  $\mu$ L media solution to which was added 95  $\mu$ L of silver colloid, which was then  
144 mechanically mixed using a micro-pipette. Each sample was measured immediately after  
145 mixing using the super macro point mode which involved the collection of seven Raman  
146 spectra (and backgrounds) from around the well center. Spectra were then co-added and each  
147 sample was measured in triplicate using fresh aliquots in different wells.

148  
149 **2.3 Chemometrics and data analysis:** All calculations were performed using PLS\_Toolbox  
150 4.0<sup>®</sup>, supplemented by in-house-written codes for Matlab<sup>®</sup> (ver. 7.4). Random spikes caused  
151 by cosmic rays were removed using an in-house written Matlab function. For the ageing  
152 experiment, any data containing cosmic spikes were immediately recollected. Classical  
153 principal component analysis (PCA) was carried out on SERS data that was baseline  
154 corrected (weighted least square algorithm) and normalized (unit area).

### 155 156 **3. Results and discussion.**

157 One of the most critical aspects in the development of a SERS based method for complex  
158 mixtures was to produce a robust sample handling procedure that delivers both signal  
159 reproducibility in terms of spectral profile and intensity, and a useful SERS enhancement  
160 with good signal-to-noise. We selected citrate reduced silver colloid [18] as this offers a  
161 good balance between ease of preparation and effective SERS response. The quality of the  
162 synthesized colloid was assessed by UV-vis spectroscopy in terms of Plasmon resonance  
163 band maximum and FWHM, which serves as an excellent diagnostic tool in lieu of measuring  
164 particle size distributions (*see supplemental information* and [24]). Once made these colloids  
165 were carefully stored in brown glass, acid washed bottles away from any direct source of  
166 light and used within 6 months of preparation. While these batches of citrate reduced colloid  
167 were suitable (as evidenced in the control sample measurements, *vide infra*) for this proof-of-  
168 concept study, we do recognize that the colloid batch reproducibility does not match the  
169 reproducibility achieved by silver colloids generated by the reduction of hydroxylamine  
170 phosphate [27]. Here to minimize the impact of colloid variation, unless stated otherwise,  
171 only one batch per experiment was used.

172 However, as important as the synthesis/storage controls, the key factors affecting the  
173 quality of the SERS spectra and data involved careful consideration/management of the  
174 sample-colloid mixture preparation step. To avoid reproducibility and background signal  
175 issues [24], we used the colloid as a suspension. Aggregation was not an issue as the eRDF  
176 formulation (17.7 g L<sup>-1</sup> soln.) contained high concentrations of aggregating agents like  
177 MgSO<sub>4</sub> (435 μM) and NaCl (105 mM). For complex media mixtures, the probability of  
178 different adsorption rates, affinities, and surface coverage for the different components was  
179 high and therefore one needed to carefully consider both the incubation time and sample-to-  
180 colloid (SC) ratio. In addition one had to account for colloid aggregation rate, which was  
181 modulated by some media components and, the time-dependent precipitation of large  
182 aggregates out of solution. The first factor increased SERS signal intensity, whereas the  
183 second reduced signal intensity.

184 *3.1 Spectral analysis:* Figure 1(top) shows the conventional Raman and SERS spectra of an  
185 eRDF solution (17.7 g L<sup>-1</sup>) and as expected the classical Raman spectra gave a very weak  
186 signal that was not very diagnostic [15]. SERS in contrast gave strong signals with multiple  
187 enhanced bands in the fingerprint region. Since eRDF was a complex mixture we get  
188 enhancement of multiple surface adsorbed species leading to this complex signal. The  
189 complexity of eRDF (with many SERS active compounds present), coupled with the different  
190 enhancement factors for each analyte made an accurate assignment of each band to a  
191 particular vibrational mode of a specific compound a challenging task (see *supplemental*  
192 *information* for more details). We suggest that, due to their structure and relatively high  
193 concentrations, most of the strong SERS signals originate from the amino acids [28-30] and  
194 vitamins present. The 1394 cm<sup>-1</sup> band was probably the amino acid –COO<sup>-</sup> symmetric  
195 stretch [31, 32], the ~914 cm<sup>-1</sup> band the C–COO<sup>-</sup> stretch, the weak band at 722 cm<sup>-1</sup> could be  
196 COO<sup>-</sup> deformation while the shoulder at 626 cm<sup>-1</sup> was probably due to COO<sup>-</sup> wag [32]. The  
197 C–S stretching of cysteine (present at 600 μM) was probably responsible for part of the 658  
198 cm<sup>-1</sup> band [33], however, it was also possible that folic acid (present at 19.94 μM) also  
199 contributed to this band and to the peak at 962 cm<sup>-1</sup>.<sup>1</sup> The broad band around 1600 cm<sup>-1</sup> was  
200 the water O–H bending mode with contributions from other modes such as ring CC stretches  
201 of aromatic amino acids. The shape of this band in particular varies significantly (*vide infra*)  
202 according to the SC ratio employed. In the context of media change identification, it was less  
203 important to identify the specific source of each band, than to observe composition change.  
204 The identification of the specific species involved in media change would be better suited to  
205 high-resolution mass spectrometry methods.

206 *3.2 Time dependence of SERS measurements:* It has been shown [19, 34] that the incubation  
207 time<sup>2</sup> can influence the profile and quality of SERS spectra. To assess the effect of different  
208 incubation times on the SERS measurement of the eRDF solution, a series of SERS spectra  
209 were collected over a 20 min incubation period using an arbitrarily chosen 1:4 SC ratio  
210 (Figure 1). This showed that the main variation observed in the SERS spectra were increases  
211 in baseline intensity and enhancement with time (Figure 2a/b). The largest increase occurred

---

<sup>1</sup> No specific vibrational mode was associated with these bands in the literature.

<sup>2</sup> Time between the moment when the sample is added to the colloid and time of the measurement.

212 during the first ~ 6 minutes, after which it slowed. The eRDF induced aggregation of the  
213 nanosized Ag colloid particles, caused at first a relatively large increase in average particle  
214 size, leading to very significant increase in the amount of Tyndall scattering from the sample,  
215 and thus an increased baseline. After this initial growth phase, the relative increase of  
216 aggregate size was much less and there were comparatively fewer particles present and thus  
217 the rate of increase in Tyndall scattering decreased.

218 When the changes in the intensity of the SERS signal due to analytes were  
219 investigated by plotting the integrated area of the baseline corrected spectra versus incubation  
220 time (Figure 2b), it was clear that the SERS enhancement followed the same trend as the  
221 baseline signal which indicated that the effects were related. This can be attributed to two  
222 factors: 1). as the colloidal particles aggregate, highly angled, contact junctions between  
223 particles were formed and these are known to generate dramatically larger SERS signals, and  
224 2). the increased aggregate size resulted in a red-shift of the Plasmon resonance closer to the  
225 excitation wavelength which further increased SERS enhancement [35].

226 The other significant aspect of the SERS spectra was the fact that the spectral profile  
227 (Figure 2C) was largely unchanged over the 20 minute incubation time which indicated that  
228 media components interacted very quickly with the Ag surface generating a stable population  
229 of surface-bound analytes. This was supported by a PCA model of the raw SERS spectra  
230 (data not shown) where only one component was needed to explain 99.85 % of the spectral  
231 variance. This showed that SERS spectral changes were related only to absolute intensity  
232 and not due to any changes in the surface bound population of analytes. Similarly, a single  
233 component PCA model fitted using baseline corrected and normalised data explaining 99.84  
234 % of the total variance. Since in both cases the explained variances were very similar and >  
235 99.8 %, this meant that the difference between the spectra collected with different incubation  
236 times was only a change in scale (multiplicative factor/signal enhancement increase with  
237 time). However, it should be noted that the SERS spectra were only this well behaved when  
238 the sample/colloid mixture was re-suspended mechanically (with a micropipette) immediately  
239 prior to measurement. If this was not done, then the presence of multiple aggregating agents  
240 in the eRDF caused rapid precipitation of colloid aggregates out of the suspension. When the  
241 incubation experiment was implemented using different SC ratios (see *SI*) similar behaviour  
242 was observed for the baseline and spectral signal intensities. However, it was also noted that  
243 the spectral profile changed significantly as the SC ratio varied.

244 *3.3 Influence of SC ratio:* The profile of the SERS spectra depends dramatically (Figure 3a)  
245 on SC ratio and SERS signal intensity was strongest for small SC ratios with intensity  
246 gradually being decreased with additional colloid. What was more important for diagnostic  
247 applications was the large spectral profile change in the normalised spectra (Figure 3b). This  
248 indicated that there were very different surface analyte populations present and thus one  
249 needed to exercise caution in selecting the correct ratio. For a 1:199 SC ratio, the relative  
250 peak intensities were much more comparable across the spectral range which might suggest  
251 that there was a much more diverse population of analytes, all of which contributed relatively  
252 equally to the SERS spectrum. Since, eRDF comprised of many different molecules with  
253 varying affinities for the Ag surface, the provision of excess colloid enabled more analyte  
254 binding and enhancement. For example the lower affinity compounds like folic acid (bands

255 at 690, 1186, 1510, and  $\sim 1595\text{ cm}^{-1}$  see *SI*) now become visible [36]. In contrast, for the  
256 larger ratios (*e.g.* more sample), it was the higher affinity components (*e.g.* cysteine, C-S  
257 stretch at  $658\text{ cm}^{-1}$  [33]) that dominate the SERS spectra because they will occupy  
258 proportionally more of the available sites. The variation in band intensities due to SC ratio  
259 changes were not linear, for example, Figure 3c plotted the  $666\text{ cm}^{-1}$  band intensity (which  
260 probably includes the cysteine C-S stretch) against SC ratio. Band intensity first rapidly  
261 increased (with a logarithmic dependence) before attaining a steady-state. It was suspected  
262 that weaker bound analytes were being displaced by a smaller range of analytes which give a  
263 stronger SERS response (*i.e.* those species which have a stronger affinity to the Ag surface).

264 Therefore, the SC ratio was critical for the analysis of complex media and the ratio  
265 selected should be such that there were sufficient binding sites available which generated a  
266 diverse and stable surface-bound population of analytes, and thus in turn led to reproducible  
267 and informative SERS spectra. This must be balanced against the loss in SERS signal  
268 intensity, increased background from particle scatter, and decreased signal-to-noise (S/N)  
269 which is a consequence of using a small SC ratio (*e.g.*  $< \sim 1:20$ ). The lower S/N resulted from  
270 first poorer aggregation because of lower levels of intrinsic aggregating agents from the cell  
271 culture media and second the lower analyte concentrations gave weaker SERS signals. One  
272 way to overcome this second point would be to add a separate aggregating agent to the  
273 sample/colloid mixture. However, this has to be carried out with care as this addition could  
274 introduce anomalies in the SERS spectra [37]. On the basis of the experimental studies  
275 (Figure 3c) we selected an SC ratio of 1:19 for the media degradation studies as this offered  
276 the best compromise in terms of S/N and spectral quality.

277 *3.4 SERS monitoring of media storage induced changes:* The validity of the storage induced  
278 changes as measured by SERS was confirmed by comparison (Figure 4) of test spectra  
279 collected on freshly prepared eRDF solutions with the control sample (stored for 32 days at –  
280  $70\text{ }^{\circ}\text{C}$ ) spectra. The plots showed that the SERS spectra did not change significantly (*e.g.* due  
281 to different colloid performance, instrument settings) over the 32 day period of the  
282 experiment. There was a small decrease in intensity for two peaks observed and this might  
283 be attributable to some variance induced during the freeze-thaw cycle. However, these were  
284 very small when compared to the differences observed due to the different storage conditions.

285 It was clear from the eRDF SERS spectra from the different storage conditions  
286 (Figure 5) that light exposure caused a great degree of spectral change. The largest light-  
287 induced change were manifested as an increased background which originated from  
288 riboflavin photo-products and its associated photosensitized degradation of other components  
289 [3-5, 7, 8, 10]. This resulted in changes in riboflavin and tryptophan, concentrations with the  
290 simultaneous formation of lumichrome [8, 11]. One potential source of baseline signal was  
291 the formation of a citrate-lumichrome complex [38], which has red fluorescence emission.  
292 The colloid used here had a significant citrate concentration (both surface bound and free in  
293 solution) which could bind to lumichrome, generating the red emitting fluorophore. A  
294 secondary source of background was variable aggregation dynamics caused by the changed  
295 chemical composition.

296 What was more interesting was the very significant changes in SERS signal for the  
297 samples dark-stored where there was no photo-degradation as shown by EEM fluorescence



298 analysis which showed virtually no change ([10, 11]). Since the control experiment (Figure  
299 4) showed minimal SERS spectral change for samples stored at  $-70\text{ }^{\circ}\text{C}$ , the obvious  
300 conclusion was that solution phase chemical reactions between media components had  
301 occurred. These changes in dark-stored media occurred in two principal regions: a loss of  
302 signal intensity in the  $660\text{-}680\text{ cm}^{-1}$  band and the appearance of two new bands in the  $1520\text{-}$   
303  $1760\text{ cm}^{-1}$  region. The interpretation of these spectral changes in terms of specific chemical  
304 constituents was not possible with a high degree of certainty because of the sample  
305 complexity and because of the convoluted interplay between selective enhancements,  
306 aggregation rates etc. In addition the presence of high aggregating agent concentrations (*e.g.*  
307 KCl, NaCl,  $\text{MgSO}_4$ , etc.) in the eRDF made definitive band assignment more problematical  
308 as it is well known that the SERS behaviour of some amino acids like cysteine can be  
309 strongly influenced by the aggregating agent [37]. However, cysteine which was present at  
310 relatively high concentration was easily oxidised to cystine in solution, particularly in the  
311 presence of ferric [39] or cupric ions (both present in eRDF). Furthermore, the SERS  
312 behaviour of cysteine/cystine shows good correlation with the changes observed here (*vide*  
313 *infra*) [28, 33, 37, 40-42]. To validate these observations we attempted to measure the  
314 cysteine concentration changes using chromatographic means [43, 44]. However, the  
315 separation of cysteine/cystine was problematical and a pre-treatment step with iodoacetic acid  
316 was required prior to the derivatisation step with PTC to obtain the S-carboxymethyl-  
317 derivative of cysteine [45] (details in *supplemental information*). This was time-consuming  
318 and in the case of the eRDF media, had a negative impact on the quality of the HPLC results.  
319 Thus it was not possible to obtain accurate cysteine concentration data from our HPLC **setup**.

320 Therefore, to better understand the source of chemical change, Principal Component  
321 Analysis (PCA) was then used to analyse the SERS spectral changes. The dark stored  
322 samples were modelled using two components (99.77 % explained spectral variance) whereas  
323 light exposed samples required three components (99.83 % explained variance). In both  
324 cases (Figure 7), the first and second PCA components were very similar (see *SI*). PC1  
325 scores increased with storage time while PC2 decreased (Figure 6) which suggested that these  
326 components were associated with the degradation product(s) and the loss of a component  
327 respectively. A possible interpretation of the variations modelled by PC1 and PC2 could be  
328 the oxidation of cysteine (PC2) and possible production of cystine (PC1). When the PC1  
329 and PC2 loadings were compared with published SERS data for both cystine and cysteine  
330 [28, 37, 40, 46] there was good agreement. In particular, the match between all the bands in  
331 PC2 and the SERS spectra of cysteine on citrate reduced silver colloids was very good [37,  
332 40] (see *SI*). We note that in PC2 we did not observe any bands around  $540\text{ cm}^{-1}$  (S-S  
333 stretch) which would indicate the presence of the cystine dimer bound to the surface [46]. In  
334 PC1, there was a broad band at  $538\text{ cm}^{-1}$  which could be the  $\nu(\text{S-S})$  vibrational mode as  
335 suggested by recent SERS studies into the behaviour of both cysteine and cystine on Au and  
336 Ag substrates [40]. The most likely explanation for these observations was that, during  
337 storage the cysteine (PC2) originally present in the medium gradually oxidises to the dimer,  
338 cystine (PC1). An alternative cysteine oxidative degradation pathway involving the  
339 generation of sulfonic acids by more extreme oxidation was studied by SERS [42]. The  
340 oxidation products (tentatively identified as sulfonic/sulfonic acids) have SERS spectra

341 similar to PC1 (see *SI*). The third possibility is that as cysteine is removed by oxidation,  
342 binding sites on the colloid are freed up thus enabling other media components with poorer  
343 affinity for the colloid to adsorb and generate a different SERS spectrum. However, on the  
344 balance of the available evidence it is the cysteine-cystine conversion that is the most  
345 probable source of the observed changes in the SERS spectra for the dark-stored samples.

346 In the case of the light exposed samples, SERS is less useful as the degradation is  
347 more easily monitored using fluorescence [11]. However, it was noted that in the PCA model  
348 of the light exposed samples that the first two components were very similar to those  
349 obtained for the dark-stored samples. The third PC in the light exposed PCA model  
350 originates from baseline effects probably induced by the photo-products (see above). It was  
351 also noted from the PCA scores (Figure 6) that the rates of change were greater in the light  
352 than for dark-stored media (see *SI* for 2D scores plots, Figure S-11). In addition, for the  
353 light-stored samples there was no observable temperature effect (Figure 6d) on the PC2  
354 scores (cysteine decrease) as was the case for the dark-stored samples (Figure 6b).

#### 355 **4. Conclusions**

356 SERS was able to detect changes in chemically defined cell culture media which  
357 occur under normal, cold, dark storage conditions. The SERS reproducibility issues was  
358 overcome by the implementation of rigorous quality control in the synthesis and handling of  
359 the citrate reduced Ag colloid, combined with a carefully designed sample incubation/data  
360 collection protocol. With these procedures we showed that substrate induced variation was  
361 much less than that caused by media ageing and thus the method was effective for media  
362 change analysis. Significant changes were observed both in irradiated and non-irradiated  
363 media which suggested that the phenomena observed by SERS were different to those  
364 observed by multi-dimensional fluorescence measurements [11]. A key conclusion was that  
365 large variations in the cell culture media chemical composition occur at an early stage with  
366 dark-stored media (within the first 5 to 10 days after preparation). The data suggests strongly  
367 that in the dark the most significant chemical change involved cysteine oxidation which takes  
368 place rapidly over the first 15 days, after which media composition stabilises. PCA of the  
369 SERS data allowed for qualitative monitoring of cysteine changes and this is useful since it is  
370 known that cysteine form promotes cell growth which is not the case for cystine [47].  
371 Furthermore, to the best of our knowledge, there is no other rapid and easy to implement  
372 technique available for monitoring this cysteine-cystine change. HPLC required intensive  
373 sample handling and preparation, and was not an easy method to implement for the  
374 quantification of cysteine-cystine and thus identification of media change. In contrast, the  
375 SERS technique presented here allows for rapid monitoring of the cysteine-cystine change  
376 with minimal sample handling and preparation. Finally, since we need neither high  
377 resolution nor sensitivity, this SERS method can be implemented using relatively low-cost  
378 bench top Raman spectrometers thus reducing the overall cost of media testing.

#### 379 **5. Acknowledgements**

380 AC acknowledges funding support from IRCSET (Irish Research Council for Science,  
381 Engineering & Technology).

#### 382 **6. Supplemental information available**

383 Supporting information is available including further details on the spectral and quantitative  
384 analyses.  
385  
386

387 **References**

- 388 [1] F. Chua, S. Oh, M. Yap, W. Teo, Enhanced IgG production in eRDF media with and  
389 without serum: A comparative study, *J Immunol Methods*, 167 (1994) 109-119.
- 390 [2] P.W. Ryan, B. Li, M. Shanahan, K.J. Leister, A.G. Ryder, Prediction of Cell Culture  
391 Media Performance Using Fluorescence Spectroscopy, *Anal. Chem.*, 82 (2010) 1311-1317.
- 392 [3] R.J. Wang, J.D. Stoen, F. Landa, Lethal Effect of Near-Ultraviolet Irradiation on  
393 Mammalian-Cells in Culture, *Nature*, 247 (1974) 43-45.
- 394 [4] R.J. Wang, Lethal Effect of Daylight Fluorescent Light on Human Cells in Tissue-  
395 Culture Medium, *Photochem. Photobiol.*, 21 (1975) 373-375.
- 396 [5] B.T. Nixon, R.J. Wang, Formation of photoproducts lethal for human cells in culture  
397 by daylight fluorescent light and bilirubin light., *Photochem. Photobiol.*, 26 (1977) 589-593.
- 398 [6] A.M. Edwards, E. Silva, B. Jofre, M.I. Becker, A.E. Deioannes, Visible-Light Effects  
399 on Tumoral Cells in a Culture-Medium Enriched with Tryptophan and Riboflavin, *J.*  
400 *Photochem. Photobiol. B-Biol.*, 24 (1994) 179-186.
- 401 [7] J.D. Stoen, R.J. Wang, Effect of Near-Ultraviolet and Visible Light on Mammalian-  
402 Cells in Culture .2. Formation of Toxic Photoproducts in Tissue-Culture Medium by  
403 Blacklight, *Proc. Natl. Acad. Sci. U. S. A.*, 71 (1974) 3961-3965.
- 404 [8] L. Zang, R. Frenkel, J. Simeone, M. Lanan, M. Byers, Y. Lyubarskaya, Metabolomics  
405 Profiling of Cell Culture Media Leading to the Identification of Riboflavin Photosensitized  
406 Degradation of Tryptophan Causing Slow Growth in Cell Culture, *Anal. Chem.*, 83 (2011)  
407 5422-5430.
- 408 [9] Y. Jing, M. Borys, S. Nayak, S. Egan, Y.M. Qian, S.H. Pan, Z.J. Li, Identification of  
409 cell culture conditions to control protein aggregation of IgG fusion proteins expressed in  
410 Chinese hamster ovary cells, *Process Biochem.*, 47 (2012) 69-75.
- 411 [10] A. Calvet, Ph.D. Chemistry, National University of Ireland Galway, Galway, 2012, p.  
412 269.
- 413 [11] A. Calvet, B. Li, A.G. Ryder, A rapid fluorescence based method for the quantitative  
414 analysis of cell culture media photo-degradation, *Anal. Chim. Acta*, 807 (2014) 111-119.
- 415 [12] R. Bro, PARAFAC. Tutorial and applications, *Chemometr. Intell. Lab. Syst.*, 38  
416 (1997) 149-171.
- 417 [13] A. de Juan, R.A. Tauler, Multivariate curve resolution (MCR) from 2000: progress in  
418 concepts and applications, *Crit. Rev. Anal. Chem.*, 36 (2006) 163-176.
- 419 [14] A.G. Ryder, J. De Vincentis, B.Y. Li, P.W. Ryan, N.M.S. Sirimuthu, K.J. Leister, A  
420 Stainless Steel Multi-Well Plate (SS-MWP) for High-Throughput Raman Analysis of Dilute  
421 Solutions, *J. Raman Spectrosc.*, 41 (2010) 1266-1275.
- 422 [15] B. Li, P.W. Ryan, B.H. Ray, K.J. Leister, N.M.S. Sirimuthu, A.G. Ryder, Rapid  
423 Characterisation and Quality Control of Complex Cell Culture Media using Raman  
424 Spectroscopy and Chemometrics., *Biotechnol. Bioeng.*, 107 (2010) 290-301.
- 425 [16] A.G. Ryder, Surface enhanced Raman scattering for narcotic detection and  
426 applications to chemical biology, *Curr. Opin. Chem. Biol.*, 9 (2005) 489-493.
- 427 [17] K. Kneipp, J. Flemming, Surface enhanced Raman scattering (SERS) of nucleic acids  
428 adsorbed on colloidal silver particles, *Journal of Molecular Structure*, 145 (1986) 173-179.

- 429 [18] P.C. Lee, D. Meisel, Adsorption and Surface-Enhanced Raman of Dyes on Silver and  
430 Gold Sols, *J. Phys. Chem.*, 86 (1982) 3391-3395.
- 431 [19] B. Li, N.M.S. Sirimuthu, B.H. Ray, A.G. Ryder, Using surface enhanced Raman  
432 scattering (SERS) and fluorescence spectroscopy for screening yeast extracts, a complex  
433 component of cell culture media., *J. Raman Spectrosc.*, 43 (2012) 1074-1082.
- 434 [20] L. Rodriguez-Lorenzo, L. Fabris, R.A. Alvarez-Puebla, Multiplex optical sensing with  
435 surface-enhanced Raman scattering: A critical review, *Anal. Chim. Acta*, 745 (2012) 10-23.
- 436 [21] B. Li, P.W. Ryan, M. Shanahan, K.J. Leister, A.G. Ryder, Fluorescence EEM  
437 Spectroscopy for Rapid Identification and Quality Evaluation of Cell Culture Media  
438 Components., *Appl. Spectrosc.*, 65 (2011) 1240-1249.
- 439 [22] C. Calvet, B. Li, A.G. Ryder, Rapid quantification of tryptophan and tyrosine in  
440 chemically defined cell culture media using fluorescence spectroscopy., *J. Pharm. Biomed.*  
441 *Anal.*, 71 (2012) 89-98.
- 442 [23] O.V. Dement'eva, V.M. Rudoy, Colloidal synthesis of new silver-based  
443 nanostructures with tailored localized surface plasmon resonance, *Colloid J.*, 73 (2011) 724-  
444 742.
- 445 [24] I.A. Larmour, K. Faulds, D. Graham, SERS activity and stability of the most  
446 frequently used silver colloids, *J. Raman Spectrosc.*, 43 (2012) 202-206.
- 447 [25] N.L. Sukhov, N.B. Ershov, V.K. Mikhalko, A.V. Gordeev, Absorption spectra of  
448 large colloidal silver particles in aqueous solution, *Russ. Chem. Bull. (Transl. of Izv. Akad.*  
449 *Nauk, Ser. Khim.)*, 46 (1997) 197-199.
- 450 [26] K.G. Stamplecoskie, J.C. Scaiano, V.S. Tiwari, H. Anis, Optimal Size of Silver  
451 Nanoparticles for Surface-Enhanced Raman Spectroscopy, *J. Phys. Chem. C*, 115 (2011)  
452 1403-1409.
- 453 [27] P. White, J. Hjortkjaer, Preparation and characterisation of a stable silver colloid for  
454 SER(R)S spectroscopy, *J. Raman Spectrosc.*, 45 (2014) 32-40.
- 455 [28] E. Podstawka, Y. Ozaki, L.M. Proniewicz, Part I: Surface-enhanced Raman  
456 spectroscopy investigation of amino acids and their homodipeptides adsorbed on colloidal  
457 silver, *Appl. Spectrosc.*, 58 (2004) 570-580.
- 458 [29] K. Sang Kyu, K. Myung Soo, S. Se Won, Surface-enhanced Raman scattering (SERS)  
459 of aromatic amino acids and their glycyl dipeptides in silver sol, *J. Raman Spectrosc.*, 18  
460 (1987) 171-175.
- 461 [30] E. Podstawka, Y. Ozaki, L.M. Proniewicz, Adsorption of S-S containing proteins on a  
462 colloidal silver surface studied by surface-enhanced Raman spectroscopy, *Appl. Spectrosc.*,  
463 58 (2004) 1147-1156.
- 464 [31] G.D. Fleming, J.J. Finnerty, M. Campos-Vallette, F. Celis, A.E. Aliaga, C. Fredes, R.  
465 Koch, Experimental and theoretical Raman and surface-enhanced Raman scattering study of  
466 cysteine, *J. Raman Spectrosc.*, 40 (2009) 632-638.
- 467 [32] S. Stewart, P.M. Fredericks, Surface-enhanced Raman spectroscopy of amino acids  
468 adsorbed on an electrochemically prepared silver surface, *Spectrochim. Acta, Part A*, 55A  
469 (1999) 1641-1660.

- 470 [33] C.Y. Jing, Y. Fang, Experimental (SERS) and theoretical (DFT) studies on the  
471 adsorption behaviors of L-cysteine on gold/silver nanoparticles, *Chem. Phys.*, 332 (2007) 27-  
472 32.
- 473 [34] Y. Chen, L. Wu, Y. Chen, N. Bi, X. Zheng, H. Qi, M. Qin, X. Liao, H. Zhang, Y.  
474 Tian, Determination of mercury(II) by surface-enhanced Raman scattering spectroscopy  
475 based on thiol-functionalized silver nanoparticles, *Microchim. Acta*, 177 (2012) 341-348.
- 476 [35] E.C. Le Ru, E. Blackie, M. Meyer, P.G. Etchegoin, Surface enhanced Raman  
477 scattering enhancement factors: a comprehensive study, *J. Phys. Chem. C*, 111 (2007) 13794-  
478 13803.
- 479 [36] R.J. Stokes, E. McBride, C.G. Wilson, J.M. Girkin, W.E. Smith, D. Graham, Surface-  
480 enhanced Raman scattering spectroscopy as a sensitive and selective technique for the  
481 detection of folic acid in water and human serum, *Appl. Spectrosc.*, 62 (2008) 371-376.
- 482 [37] N.R. Yaffe, E.W. Blanch, Effects and anomalies that can occur in SERS spectra of  
483 biological molecules when using a wide range of aggregating agents for hydroxylamine-  
484 reduced and citrate-reduced silver colloids, *Vibrational Spectroscopy*, 48 (2008) 196-201.
- 485 [38] Z. Miskolczy, L. Biczok, Anion-induced changes in the absorption and fluorescence  
486 properties of lumichrome: A new off-the-shelf fluorescent probe, *Chem. Phys. Lett.*, 411  
487 (2005) 238-242.
- 488 [39] R.F. Jameson, W. Linert, A. Tschinkowitz, Anaerobic Oxidation of Cysteine to  
489 Cystine by Iron(III) .2. The Reaction in Basic Solution, *J. Chem. Soc.-Dalton Trans.* (1988)  
490 2109-2112.
- 491 [40] E. Lopez-Tobar, B. Hernandez, M. Ghomi, S. Sanchez-Cortes, Stability of the  
492 Disulfide Bond in Cystine Adsorbed on Silver and Gold Nanoparticles As Evidenced by  
493 SERS Data, *J. Phys. Chem. C*, 117 (2013) 1531-1537.
- 494 [41] A.G. Brolo, P. Germain, G. Hager, Investigation of the adsorption of L-cysteine on a  
495 polycrystalline silver electrode by surface-enhanced Raman scattering (SERS) and surface-  
496 enhanced second harmonic generation (SESHG), *J. Phys. Chem. B*, 106 (2002) 5982-5987.
- 497 [42] C.V. Stevani, D.L.A. de Faria, J.S. Porto, D.J. Trindade, E.J.H. Bechara, Mechanism  
498 of automotive clearcoat damage by dragonfly eggs investigated by surface enhanced Raman  
499 scattering, *Polym. Degrad. Stabil.*, 68 (2000) 61-66.
- 500 [43] V.P. Hanko, J.S. Rohrer, Determination of amino acids in cell culture and  
501 fermentation broth media using anion-exchange chromatography with integrated pulsed  
502 amperometric detection, *Analytical biochemistry*, 324 (2004) 29-38.
- 503 [44] J.A. White, R.J. Hart, J.C. Fry, An Evaluation of the Waters PICO-TAG System for  
504 the Amino-Acid-Analysis of Food Materials, *J. Autom. Chem.*, 8 (1986) 170-177.
- 505 [45] L. Campanella, G. Crescentini, P. Avino, Simultaneous determination of cysteine,  
506 cystine and 18 other amino acids in various matrices by high-performance liquid  
507 chromatography, *J. Chromatogr. A*, 833 (1999) 137-145.
- 508 [46] G. Diaz Fleming, J.J. Finnerty, M. Campos - Vallette, F. Célis, A.E. Aliaga, C.  
509 Fredes, R. Koch, Experimental and theoretical Raman and surface - enhanced Raman  
510 scattering study of cysteine, *J. Raman Spectrosc.*, 40 (2009) 632-638.

511 [47] M.W. Glacken, E. Adema, A.J. Sinskey, Mathematical descriptions of hybridoma  
512 culture kinetics: II. The relationship between thiol chemistry and the degradation of serum  
513 activity, *Biotechnol. Bioeng.*, 33 (1989) 440-450.

514

515

### 516 **List of Figures & Legends.**

517

518 **Figure 1:** (top) Raw Raman spectra of *a*) milli-Q® water, *b*) a 17.7 g/L eRDF solution, and  
519 *c*). raw SERS spectrum of a 17.7 g/L eRDF solution with an SC ratio of 1:19. All three  
520 spectra were collected using identical collection conditions; (bottom) Plot of raw SERS  
521 spectra collected every minute (for 20 minutes) after mixing from samples with a SC ratio of  
522 1:4 (see text). The sample-colloid mixture was re-suspended between each measurement and  
523 the average spectra of three replicates are plotted.

524

525 **Figure 2:** Change in the SERS spectra of a 17.7 g/L solution eRDF with incubation time.  
526 (a) Change in the baseline intensity of SERS spectra (average of the data points between  
527 1802 and 2002  $\text{cm}^{-1}$ ); (b) Change in the integrated spectral area (250 to 2714  $\text{cm}^{-1}$ ) of the  
528 baseline corrected spectra. Data shown is for three replicate measurements; (c) Plot of the  
529 overlaid baselined corrected and normalised SERS spectra of all 60 spectra. The SERS were  
530 spectra collected every minute after incubation for up to 20 minutes on samples with an SC  
531 ratio of 1:4. The sample-colloid mixture was re-suspended between each measurement.

532

533 **Figure 3:** Baseline corrected (a), and baseline corrected and normalised to unit area (b)  
534 SERS spectra of eRDF (17.7 g/L) samples with 1:1 (black, batch 1 colloid), 1:9 (grey, batch  
535 3/4 colloid) and 1:199 (grey, batch 2 colloid), ratio (v/v) of sample to colloid; (c) SERS  
536 intensity of the 666  $\text{cm}^{-1}$  peak plotted against SC ratio. The line shows the logarithmic fit:  $y$   
537  $= 3168.2 \times \log(x) + 16663$ ,  $R^2 = 0.981$ . The small deviations from the log fit are probably due  
538 to the use of three different colloid batches and the intrinsic synthesis variation.

539

540 **Figure 4:** Overlap of day0 (grey) and control sample (black) raw (a) and baseline corrected  
541 and normalised (b) SERS spectra collected in triplicate.

542

543 **Figure 5:** Raw SERS spectra collected from eRDF solutions (17.7 g/L) stored under various  
544 conditions: (a) C-D; (b) RT-D; (c) C-L, and (d) RT-L. The storage time increases from  
545 black to light grey and the average spectra of three replicate are plotted.

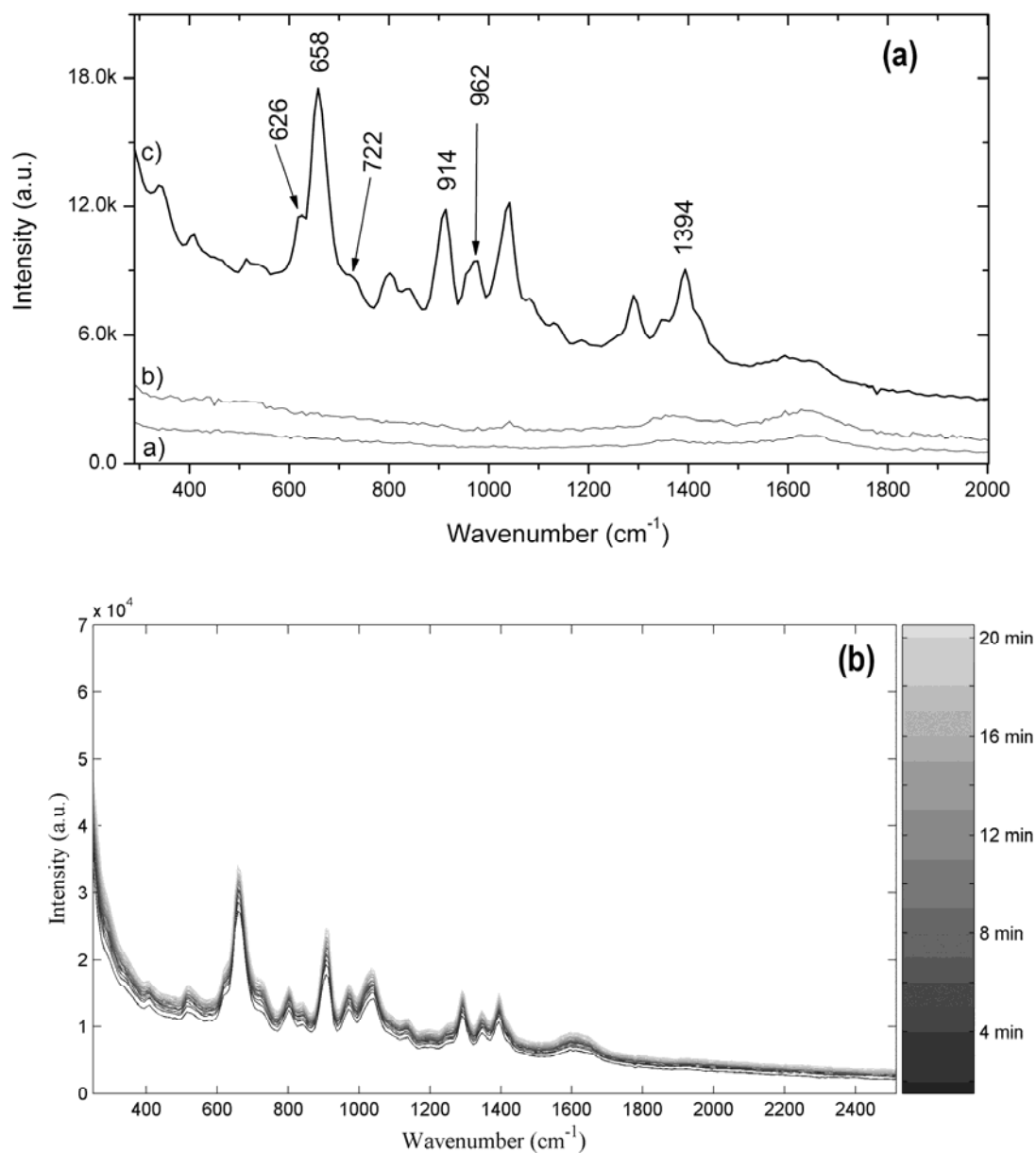
546

547 **Figure 6:** Plots of changes in the individual principal component scores versus time  
548 generated by various PCA models: (a) PC1, and (b) PC2 component scores plotted versus  
549 time at room temperature ( $\circ$ ) and in the fridge ( $\square$ ) for the dark stored samples. (c) PC1, (d)  
550 PC2, and (e) PC3 component scores plotted versus time at room temperature ( $\circ$ ) and in the  
551 fridge ( $\square$ ) for the light stored samples. PC1 vs. PC2 scores plots are available in the  
552 *supplemental information*, Figure S-11.

553

554 **Figure 7:** Loadings of the components generated by the PCA analysis of the data collected  
555 on the samples stored in the dark (a) and in the light (b) under both the cold and room  
556 temperature storage conditions.

557  
558  
559



560  
561  
562  
563  
564

**Figure 1.**



565

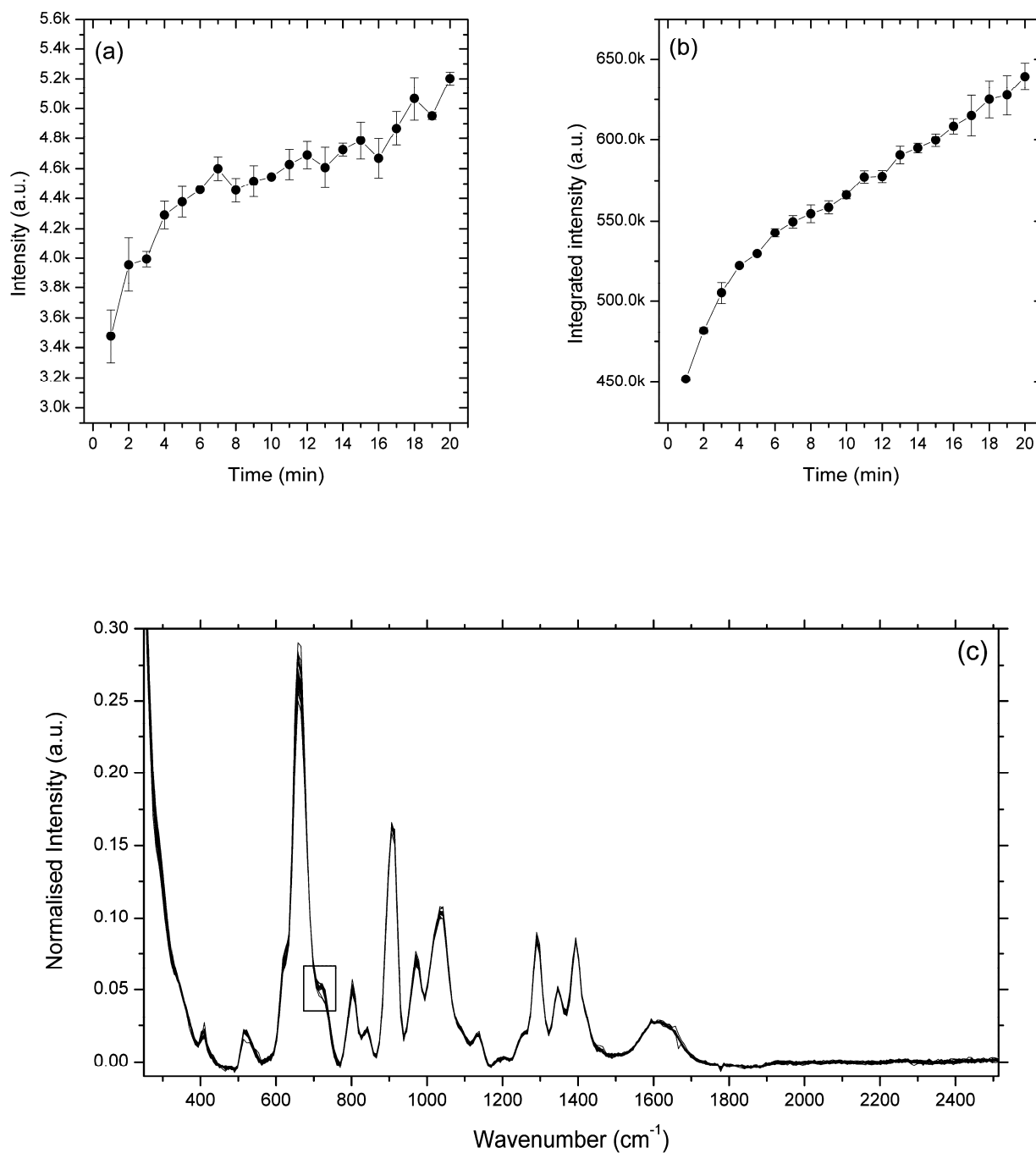
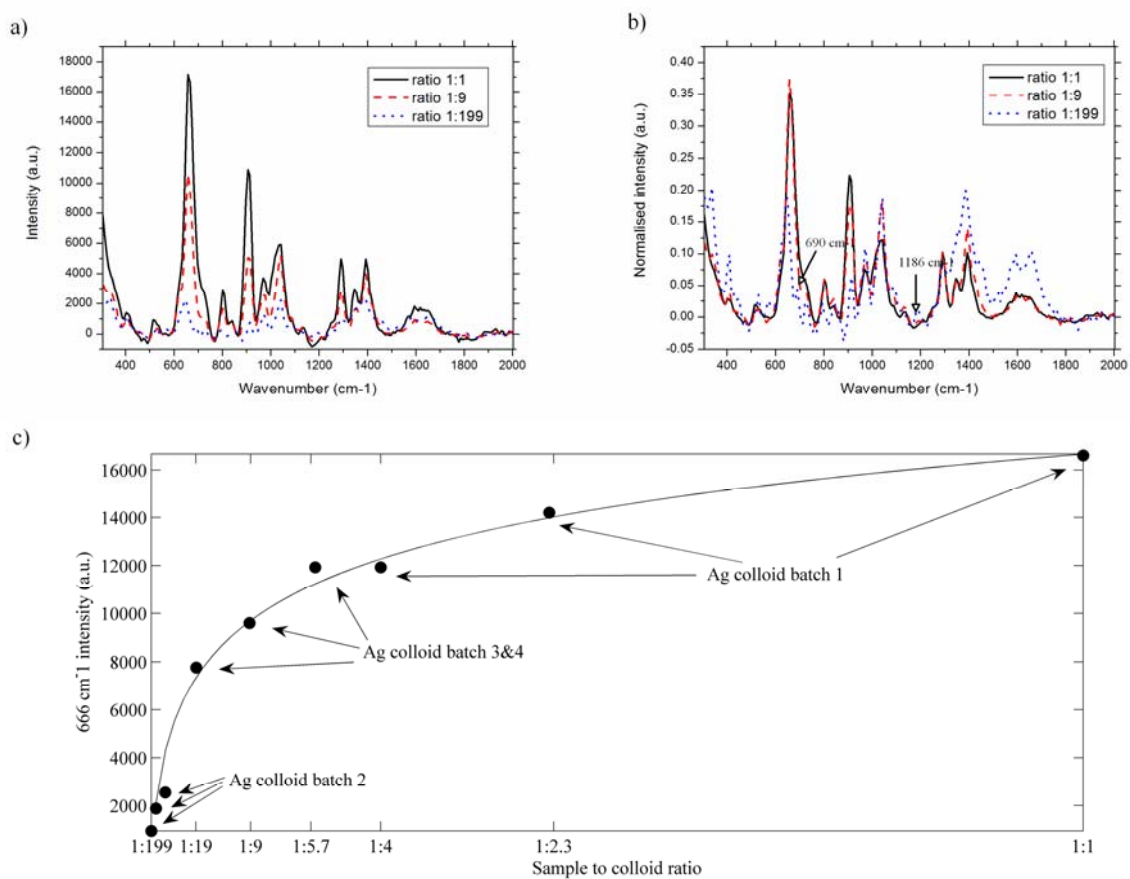


**Figure 2:**

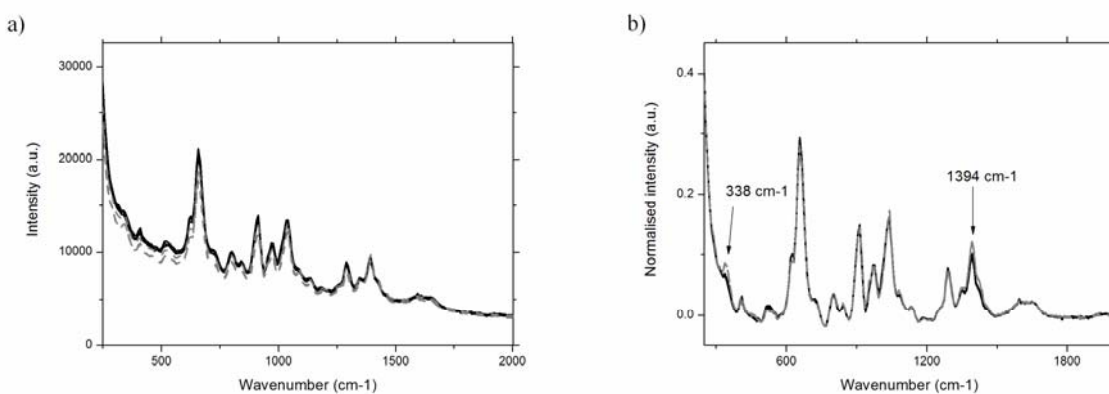
566  
567  
568  
569

570



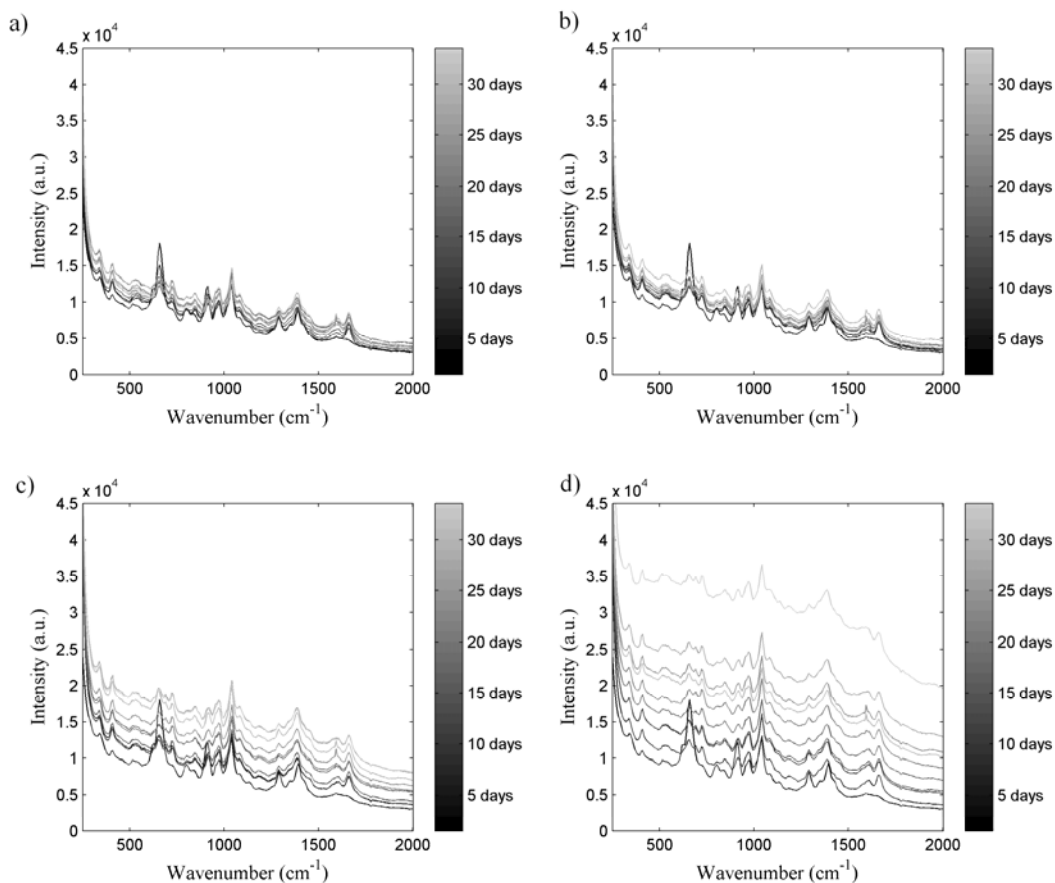
571  
572  
573  
574

**Figure 3:**



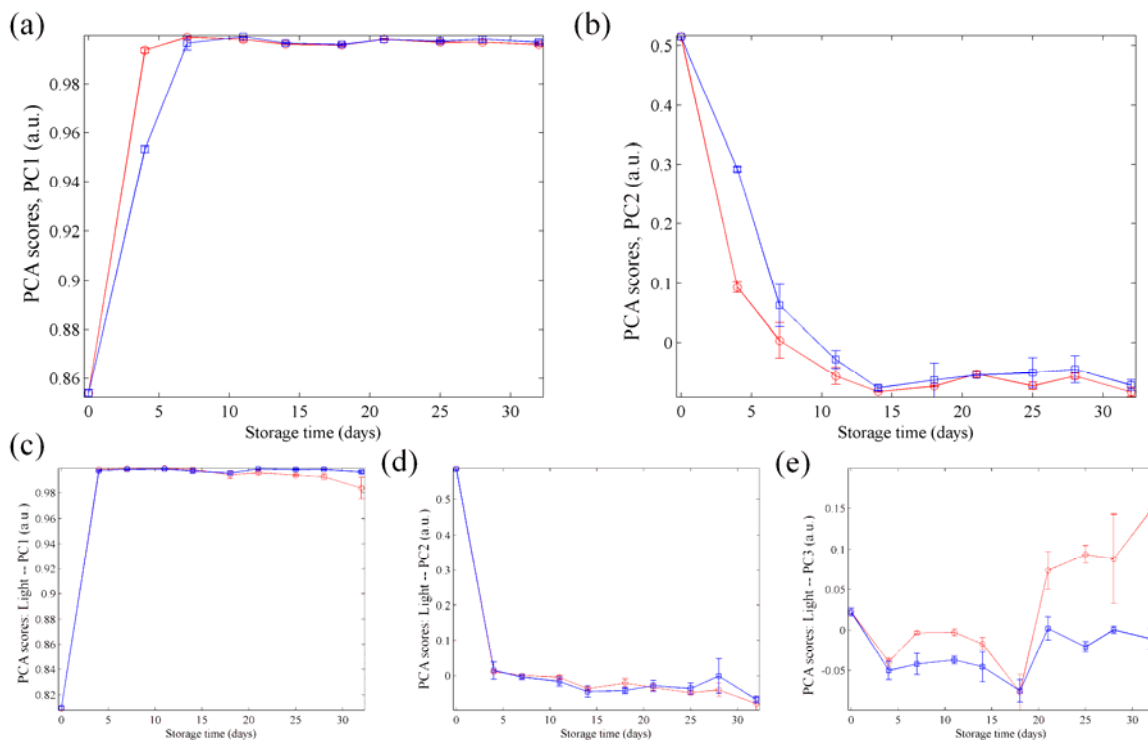
575  
576  
577  
578  
579

**Figure 4:**



580  
581

Figure 5.



582  
583

Figure 6.

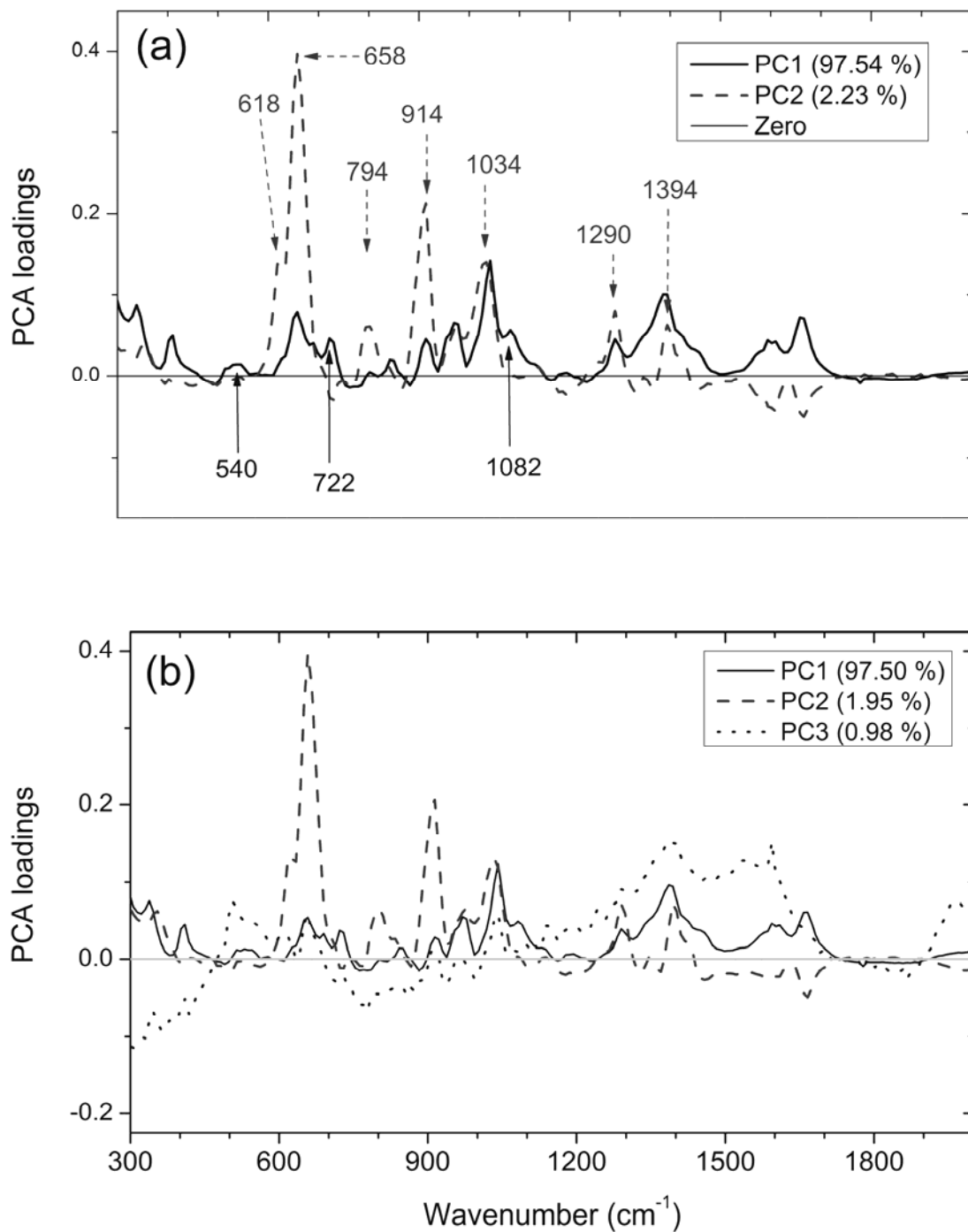


Figure 7.

584  
585